

## hcp-to-fcc stacking switch in thin cobalt films induced by Cu capping

Ch. Rath

*Lehrstuhl für Festkörperphysik, Universität Erlangen-Nürnberg, Staudtstr. 7, D-91058, Erlangen, Germany*

J. E. Prieto

*Departamento de Física de la Materia Condensada, Universidad Autonoma de Madrid, Canto blanco, E-28049 Madrid, Spain*

S. Müller

*Lehrstuhl für Festkörperphysik, Universität Erlangen-Nürnberg, Staudtstr. 7, D-91058, Erlangen, Germany*

R. Miranda

*Departamento de Física de la Materia Condensada, Universidad Autonoma de Madrid, Canto blanco, E-28049 Madrid, Spain*

K. Heinz

*Lehrstuhl für Festkörperphysik, Universität Erlangen-Nürnberg, Staudtstr. 7, D-91058, Erlangen, Germany*

(Received 24 October 1996)

We report on surface structure analyses by quantitative low-energy electron diffraction for ultrathin films of 1.5 and 5 ML Co on Cu(111) and on the structural changes they undergo when additionally covered by 2–3 ML copper. The thin cobalt film is dominated by continuation of the fcc stacking dictated by the substrate whereby a large part of the domains is capped by copper dissolved from the substrate and possibly substituted by cobalt. Yet, some stacking faults near the interface appear already at this low coverage in domains uncapped by copper. The 5 ML Co film, on the other hand, is almost fully hexagonally close packed. While the stacking of the thinnest film is practically stable upon further copper deposition, the sandwiching of the thicker film induces a structural switch from hcp to fcc stacking, whereby twinned fcc domains develop. At least one of the cobalt layers undergoes a full registry shift upon the sandwiching process. This shows that copper deposited on top of cobalt not only stabilizes the initial fcc stacking of cobalt but also can induce a switch from an existing hcp stacking of a thicker cobalt film back to fcc. [S0163-1829(97)08716-X]

### I. INTRODUCTION

Recent years have seen a steadily increasing number of papers on epitaxial metallic thin films triggered by their unusual magnetic properties as enhanced magnetic moments, magnetic anisotropy, or giant magnetoresistance (GMR). The formation of fcc Fe on Cu(100) as well as of fcc Co both on Cu(100) and Cu(111) belong to the most frequently investigated systems. In both cases the high-temperature fcc equilibrium phases can be epitaxially stabilized at room temperature and below. Because of the intrinsic coupling between structure and magnetism many efforts have been spent in retrieving the structure and morphology of the films. For Co/Cu(111), on which we focus in the present paper, many different surface structure sensitive techniques have been applied such as visual low-energy electron diffraction (LEED),<sup>1–3</sup> angle-resolved photoelectron diffraction,<sup>2–5</sup> Auger electron forward scattering,<sup>3</sup> scanning tunneling microscopy (STM),<sup>6,7</sup> thermal energy atom scattering,<sup>8</sup> low-energy ion scattering,<sup>9</sup> angle-resolved secondary electrons backscattering,<sup>10</sup> x-ray-absorption fine-structure measurements (EXAFS),<sup>11,12</sup> and quantitative LEED.<sup>8,13,14</sup> Structural information for Co/Cu(111) superlattices has been obtained by nuclear magnetic resonance (NMR) experiments<sup>15–18</sup> and x-ray diffraction.<sup>17–20</sup>

The precise determination of the stacking sequence of (111) planes in Co/Cu multilayers or superlattices has been

an important topic since it was demonstrated that stacking faults are responsible for reducing the GMR effect in sputtered Cu/Cu(111) multilayers.<sup>21</sup> Today, there appears to be overall agreement that the early stages of the epitaxial growth of Co on Cu(111) up to 2 ML are dominated by fcc cobalt, which is formed by epitaxial continuation of the fcc (111) substrate lattice with only a small density of stacking faults. Domains with mere Co double layers coexist with such capped with Cu atoms having diffused to the surface. Their relative weights determined by quantitative LEED agree with those seen in STM.<sup>13</sup> With coverage increasing beyond 2 ML, stacking faults are introduced and the film gradually transforms to hcp stacking, whereby details of the film preparation procedure and the crystallographic quality of the substrate seem to be of considerable influence.<sup>4</sup> Simultaneous with increasing hcp stacking, copper-capped domains disappear,<sup>9,13</sup> as diffusion of copper to the top becomes more unlikely with growing film thickness. Since the fcc-to-hcp transition takes place at relatively low Co coverages it is somewhat surprising that Co/Cu(111)-oriented superlattices quite often are reported to be exclusively (or mostly) fcc stacked.<sup>15–20</sup> For instance, x-ray diffraction studies found that fcc stacking of Co is predominant up to Co film thicknesses of at least 40 Å, though a considerable part of Co is found to be hcp.<sup>19</sup> NMR investigations of superlattices up to Co film thicknesses of 65 Å find only very small fractions of hcp and little mixing of cobalt and copper

equivalent to a relatively sharp interface.<sup>16</sup>

The hcp stacking of the Co film increasing with the film thickness on the one hand and the stabilization of substrate dictated fcc stacking by capping Cu atoms or a Cu film on the other hand pose some interesting questions: What is the structure of a cobalt film (>2 ML coverage) if it is covered by another copper film, thus forming a Cu/Co/Cu sandwich? Does the once established structure (layer stacking) of the Co film remain unaffected upon Cu deposition or is it induced to change due to the new structural and/or electronic boundary conditions? These questions, which were mentioned earlier to be important issues<sup>2,4</sup> and which are interesting also from the fact that sandwich structures are the building blocks of superlattices, are addressed in the present paper by means of quantitative LEED measurements and their full dynamical analysis. LEED intensity versus energy spectra,  $I(E)$ , is extremely sensitive to layer stacking sequences and stacking faults, as is well known generally and has been checked quantitatively in particular for the system Co/Cu(111) recently.<sup>22</sup> So, quantitative LEED seems to be an appropriate tool to answer the above questions.

We prepared two ultrathin Co films with different thicknesses on Cu(111), i.e., at 1.5 and 5 ML Co coverage. After the measurement of  $I(E)$  spectra the films were covered with 2–3 ML of Cu and the intensity spectra were taken again. The four sets of data were analyzed to retrieve the structure of the film, in particular the structural changes upon Cu deposition. The two Co film thicknesses are chosen because dominating fcc stacking is expected in the case of the 1.5 ML film, while it turns out that hcp stacking dominates at 5 ML when growth takes place on a substrate with large terraces, i.e., a small density of steps.<sup>23</sup> So, with no or little structural change upon Cu deposition expected for the 1.5 ML film, this serves as a test case for the more interesting investigation of the 5 ML Co film.

The paper is organized as follows. In Sec. II details of the film preparation as well as of the measurement and calculation of LEED intensities are presented. Section III gives the results for the 1.5 ML Co film, Sec. IV those for the 5 ML Co film. A conclusive discussion of all results is presented in the last section.

## II. FILM PREPARATION, INTENSITY MEASUREMENTS, AND CALCULATIONS

The experiments were carried out in a standard UHV chamber equipped with a rear-view four-grid LEED optics, which simultaneously served as a spectrometer for Auger electron spectroscopy (AES). The Cu(111) sample was cleaned by repeated argon ion sputtering followed by annealing. Deposition of cobalt and copper was made from two different reservoirs of the respective elements by evaporation through electron bombardment with a rate of about 1 ML/min, whereby the sample was kept at room temperature. The developing LEED patterns always were of  $1 \times 1$  symmetry with little background.

The deposited Co coverage was determined from the ratio of the high-energy Auger peaks,  $\text{Cu}_{920}/\text{Co}_{716} = S \alpha_{\text{Cu}}^n / (1 - \alpha_{\text{Co}}^n)$ , where  $S = \text{Cu}_{920}^\infty / \text{Co}_{716}^\infty$  is the ratio of signals from the bulk crystals determined to be in the same conditions,  $S = 1.2$ . The quantity  $\alpha_{\text{Cu}}^n$  describes the experimental attenu-

ation of the Cu signal across  $n$  layers of Co ( $\alpha_{\text{Cu}} = 0.77$ ), while  $\alpha_{\text{Co}}^n$  stands for the corresponding attenuation of the Co signal ( $\alpha_{\text{Co}} = 0.72$ ). The attenuation factor for a given Auger peak derives from the inelastic mean free path  $\lambda$  of electrons of the corresponding energy as  $\alpha = \exp(-a/0.8\lambda)$ , whereby  $a$  is the monolayer thickness. In the case of a sandwich of  $m$  layers of Cu on top of  $n$  layers of Co deposited on Cu(111), the corresponding expression is  $\text{Cu}_{920}/\text{Co}_{716} = S \alpha_{\text{Cu}}^{n+m} (1 - \alpha_{\text{Cu}}^m) / \{(1 - \alpha_{\text{Co}}^n) \alpha_{\text{Co}}^n\}$ . Similar relations were used for the ratio of the low-energy Auger peaks (Co: 53 eV; Cu: 61 eV) with consistent results. The accuracy of the coverage determination is estimated to be about  $\pm 0.3$  ML.

Intensity versus energy spectra,  $I(E)$ , were taken at room temperature using a computer controlled video method providing fast measurements with automated background subtraction minimizing the influence of residual gas adsorption after film preparation.<sup>24–26</sup> Normal incidence of the primary beam was carefully adjusted by quantitative comparison of spectra of symmetrically equivalent beams using the Pendry  $R$  factor.<sup>27</sup> The eventual adjustment reached is mirrored by Pendry  $R$  factors  $R \leq 0.04$  between equivalent beams. Further improvement of the quality of the data with respect to residual misalignment, possible screen inhomogeneities, and noise was achieved by averaging equivalent spectra prior to input to the analysis.

Standard computer codes were applied for the full dynamical analysis of the measured intensities.<sup>28,29</sup> The highest electron energy evaluated was 400 eV for which a maximum of 11 phase shifts for both copper and cobalt proved to be sufficient. They were calculated relativistically and corrected for thermal vibrations, which were assumed to be isotropic according to Debye temperatures of 343 and 445 K for copper and cobalt, respectively.<sup>30</sup> The vibrational amplitudes were varied for top layers in each case. Layer diffraction matrices were calculated by matrix inversion in angular momentum representation and layers were stacked using the layer-doubling scheme. Electron attenuation was simulated by an energy-independent imaginary part of the inner potential  $V_{0i}$ , which, together with its real part  $V_{0r}$ , was varied in the course of the theory-experiment fit. One can determine whether a layer is made up of cobalt or copper by the different atomic scattering of the two elements. As both their total cross sections e.g., at 80 eV ( $\sigma_{\text{Co}} = 2.45 \times 10^{-20} \text{ m}^2$ ,  $\sigma_{\text{Cu}} = 1.97 \times 10^{-20} \text{ m}^2$ ) and angular dependences of the differential cross sections (see Fig. 1) are quite similar, the elemental resolution is limited to the first two layers at most. This is different from the sensitivity with respect to the layer stacking. As shown below, the latter can be determined down to the fourth layer. The close fit between experimental and model intensities, which can be achieved in each case, additionally allows the precise determination of the layer spacings and in-plane lattice parameters.

The search for the correct structure is complicated by the possible appearance of different structural domains, i.e., domains with different stacking sequences of layers and different chemical composition, e.g., with and without capping by copper for the nonsandwiched films. For a single domain, the number of structural parameters is rather limited; i.e., there are only about three interlayer distances to be varied. This can be done conventionally, i.e., by the calculation of inten-

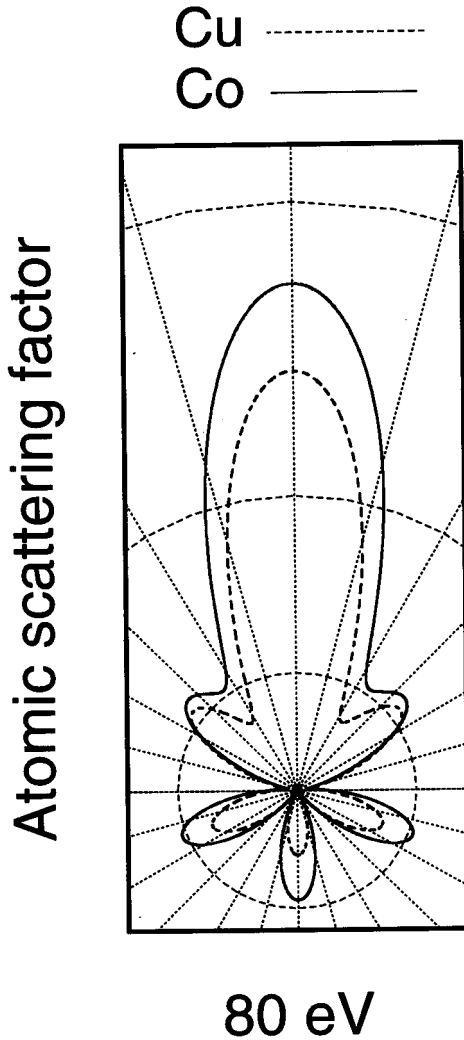


FIG. 1. Polar plot of differential scattering cross sections of electrons for both Co and Cu.

sities at each trial value of each layer separation according to a preselected grid of values. With, e.g., 10 trial values for each distance  $10^3$  trial structures result, an amount that still can be handled easily. Yet, already with two different domains present the number of trial structures to be tested is already  $(10^3)^2 = 10^6$ . It is clear that with even more domains possible and with their relative weights additionally to be varied, a grid search becomes impractical. Therefore, for the determination of the different domains and their relative weights we used an automated optimization of the theory-experiment fit that resulted from a modified random sampling algorithm discussed in detail elsewhere.<sup>31</sup> In addition to the determination of the different domains with their stacking sequences and chemical composition, we also varied the in-plane lattice parameter for each film in order to check whether the epitaxial growth is strictly pseudomorphic or if relaxation has already taken over. The Pendry  $R$  factor<sup>27</sup> was used for the quantitative comparison of experimental and calculated data in order to guide the search procedure. By the variance of the  $R$  factor,  $\text{var}(R) = R_{\min}(8V_{0i}/\Delta E)^{1/2}$  with  $R_{\min}$  the minimum  $R$  factor and  $\Delta E$  the energy width of the database, error limits due to statistical errors of measure-

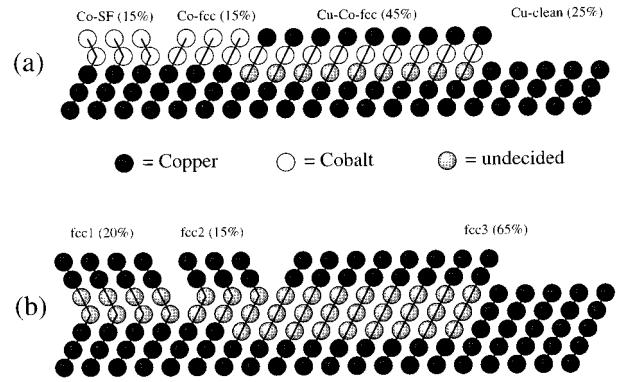


FIG. 2. Schematic structures of the epitaxial film (a) 1.5 ML Co/Cu(111) and the sandwich system (b) 3 ML Cu/1.5 ML Co/Cu(111) (SF denotes stacking fault). Atomic symbols labeled “undecided” indicate that LEED could not decide safely on the chemical nature of the respective atoms.

ment were derived for the structure parameters determined. With  $R_{\min}$  being of the order of 0.1 and  $\Delta E$  of the order of  $10^3$  eV for the different epitaxial systems investigated, rather small error limits result.

It is worth mentioning that structure analyses by LEED are practically blind with respect to the morphology of the films grown, i.e., to the height distribution of the different domains possibly present. This is at least when—as in the present case—the diffraction patterns are characterized by only little diffuse background and relatively sharp spots, indicating that the ordered domains from which the intensities are formed are not much smaller than the electron coherence length, i.e., about  $100 \text{ \AA}$  or 40 atomic diameters, or are statistically distributed. Then just the intensities add and our structural parameters derived are averages with respect to such domains. The real-space morphology of the film can be characterized quantitatively by *in situ* STM imaging<sup>13</sup> exhibiting different heights as indicated in Fig. 4(a).

### III. STRUCTURES OF THE 1.5 ML Co/Cu(111) FILM AND OF THE SANDWICH 3 ML Cu/1.5 ML Co/Cu(111)

#### A. The 1.5 ML Co/Cu(111) film

A film of this coverage was already the subject of an earlier investigation by our group,<sup>13</sup> whereby, however, a substrate with a non-negligible density of steps was used. As the substrate quality seems to play an important role in the film growth,<sup>4</sup> we decided to repeat the structure determination for the more perfect substrate. Also, it is important to know precisely the structure of the very film on which further Cu deposition is made to form a sandwich. As it turns out, the structural result is not very different from the earlier investigation. Deposition of 1.5 ML of Co on the copper substrate results in domains with uncovered Co double layers, Co layers capped with Cu atoms, and uncovered Cu(111) patches. As schematically displayed in Fig. 2(a) and also given in Table I, the uncovered area amounts to 25% of the surface. This is in perfect agreement with our earlier STM investigations.<sup>13,14</sup> In the present case the relative areas of Co double layers and Co layers capped with Cu are 30% and 45%, respectively. If we assume that the copper-covered cobalt layers are also Co double layers with the first layer em-

TABLE I. Best-fit structural parameters for the epitaxial film 1.5 ML Co/Cu(111) according to the model given in Fig. 2(a) (SF denotes stacking fault). The quantity  $a_p$  was taken from a fit carried out in earlier work (Ref. 13).

	1.5 ML Co			
	Domains Co-SF	Domains Co-fcc	Domains Cu-Co-fcc	Domains Cu-clean
Weight (%)	$15 \pm 10$	$15^{+20}_{-15}$	$45^{+15}_{-10}$	$25 \pm 20$
$d_{12}$ (Å)	$2.00 \pm 0.04$	$2.06 \pm 0.04$	$2.00 \pm 0.03$	$2.07 \pm 0.04$
$d_{23}$ (Å)	$2.01 \pm 0.06$	$2.07 \pm 0.06$	$2.07 \pm 0.04$	$2.08 \pm 0.05$
$d_{34}$ (Å)	$2.08 \pm 0.10$	$2.10 \pm 0.09$	$2.08 \pm 0.06$	2.08 (not varied)
$a_p$ (Å)	2.55	2.55	2.55	2.55
$R_{\min}$			0.12	
var( $R$ )			0.024	

bedded in the substrate and the respective copper atoms having moved to the top, exactly the total coverage of 1.5 ML results. However, as mentioned in the preceding section this value is uncertain by  $\pm 0.3$  ML and, as also emphasized, we have no safe elemental resolution with respect to atoms in the third layer. So, this feature of the structural model remains a bit speculative, though consistent. This is indicated in Fig. 2 by lightly shaded atomic symbols for atoms below the second layer, except when we have good reason to believe that atoms belong to the copper substrate. The quality of the experiment-theory fit corresponds to an all-beams averaged Pendry  $R$  factor  $R_{\min} = 0.12$  and can be judged visually for some selected beams in Fig. 3(a). Other beams compare on the same level of agreement. The error limits given in Table I result from the variance of the  $R$  factor,  $\text{var}(R) = 0.023$ . The table also displays the interlayer distances for each domain. On the basis of the systematic variation of the

in-plane lattice parameter carried out in our earlier investigation,<sup>13</sup> the in-plane lattice parameter of the copper substrate (2.55 Å) could also be used for the film.

The most important structural result of the 1.5-ML film analysis is, however, that in as much as 60% of the surface, deposited Co atoms and/or Cu atoms moved to the top have continued the fcc stacking of the copper substrate. This is, of course, in agreement with the experimentally observed three-fold symmetry of the diffraction pattern and is in line with earlier results.<sup>13</sup> Yet, even at the low coverage of 1.5 ML some small areas (15%) of Co double layers exhibit a stacking fault that is likely to trigger further growth with hcp stacking. According to molecular-dynamics simulations for Cu adatoms moving on Cu(111),<sup>32</sup> the fcc site is more stable than the hcp site by only 17 meV. Although to our knowledge there are no calculations for Co on Cu(111), one may safely assume that the energy difference in this case will also be small enough to justify the existence of nucleation at both sites at room temperature. Though the existence of stacking faults is near the limits of error (see Table I), the present crystallographic results seem to be slightly different from the above-mentioned earlier investigations<sup>13,14</sup> at 1.5-ML coverage on a substrate with a non-negligible number of steps. This seems to confirm the suggestion that the details of the growth, such as substrate quality, evaporation rate, or time between deposition and observation are of some influence for the initial stacking sequence.<sup>4</sup>

### B. The sandwich 3 ML Cu/1.5 ML Co/Cu(111)

Upon deposition of 3 ML copper on the above film the threefold symmetry of the diffraction pattern remains. The  $I(E)$  spectra undergo some undramatic changes. This indicates that fcc stacking remains dominant and possible fcc twins do not develop with equal weight. Nevertheless, we allowed for such twinned domains with variable weights in the structural search together with the appearance of stacking faults, in particular at or near the two interfaces. Also, the stacking of the former unsandwiched film was allowed to change. The eventually retrieved best-fit structure is displayed schematically in Fig. 2(b). We remind the reader that the chemical specificity of our LEED analysis is not sufficient to determine the nature of atoms below the second layer. The minimum  $R$  factor is very low again ( $R_{\min}$

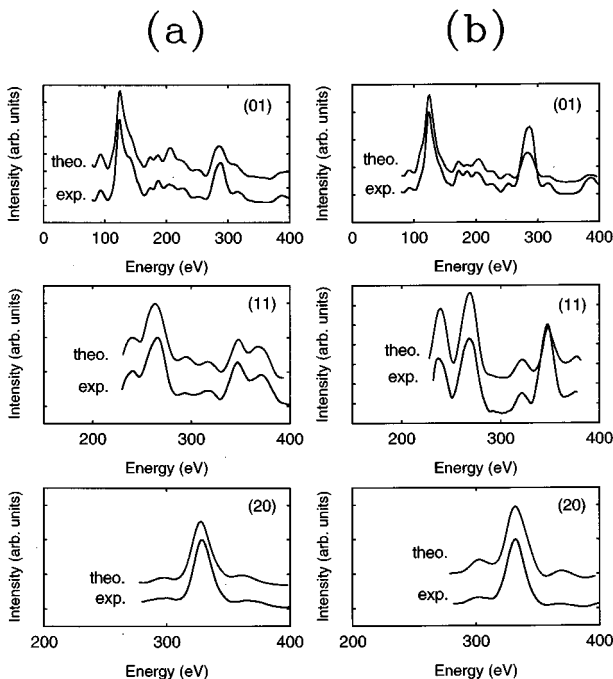


FIG. 3. Comparison of best-fit calculated and experimental spectra for three selected beams of the film (a) 1.5 ML Co/Cu(111) and the sandwich system (b) 3 ML Cu/1.5 ML Co/Cu(111).

TABLE II. Best-fit structural parameters for the sandwich 3 ML Cu/1.5 ML Co/Cu(111) according to the model given in Fig. 2(b).

	3 ML Cu/1.5 ML Co		
	Domains fcc1	Domains fcc2	Domains fcc3
Weight (%)	$20 \pm 10$	$15^{+15}_{-10}$	$65 \pm 10$
$d_{12}$ (Å)	$2.02 \pm 0.03$	$2.08 \pm 0.04$	$2.06 \pm 0.02$
$d_{23}$ (Å)	$2.04 \pm 0.04$	$2.04 \pm 0.05$	$2.08 \pm 0.03$
$d_{34}$ (Å)	$2.10 \pm 0.06$	$2.10 \pm 0.05$	$2.08 \pm 0.05$
$a_p$ (Å)	$2.55^{+0.020}_{-0.025}$	$2.55 \pm 0.035$	$2.55^{+0.015}_{-0.025}$
$R_{\min}$		0.10	
var( $R$ )		0.020	

=0.10) with a variance of  $\text{var}(R)=0.020$ , and experimental and best-fit model spectra also compare extremely well visually [Fig. 3(b)].

The overall result of the analysis is that the stacking of at least the top three layers is fcc, whereby twinned domains with unequal weights (35% and 65%) coexist. Not surprisingly the additionally deposited copper continues the dominating fcc stacking of the predeposited cobalt albeit twinned. As displayed in Fig. 2(b), stacking faults at or near the lower Co-Cu interface remain and some more develop. Yet, it seems to be clear that no stacking faults with respect to fcc stacking are found more distant from the interface.

The quantitative structural parameters of the best-fit model including the error limits are given in Table II. The lateral lattice parameter, which was additionally varied, is the same as that for the clean Cu(111) surface in all domains,  $a_p=2.55$  Å. As expected for close-packed surfaces, there are no considerable relaxations of interlayer distances. Instead, within the limits of error the distances are all the same and close to both the bulk values of Co(0001) and Cu(111), i.e., 2.05 and 2.09 Å, respectively.

#### IV. STRUCTURES OF THE 5 ML Co/Cu(111) FILM AND OF THE SANDWICH 2 ML Cu/5 ML Co/Cu(111)

##### A. The 5 ML Co/Cu(111) film

The morphology of the 5 ML Co film corresponds to a Poisson distribution of layer population above the first bilayer leading to pyramid-shaped islands as found from STM images<sup>6,7</sup> and schematically displayed in Fig. 4(a). Different from the 1.5 ML Co/Cu(111) film the diffraction pattern of the 5 ML Co film exhibits nearly, though not ideally sixfold rotational symmetry. This could be due to the existence of equally weighted domains of either fcc twins or hcp stacked areas separated by monoatomic steps. Without any doubt the analysis identifies the latter case to be true. The small deviation from ideal sixfold symmetry could come from either not strictly equally weighted hcp domains or some residual fcc stacking. Again the latter case is true as can be identified by the small statistical error limits [ $\text{var}(R)=0.014$ ], which come through the excellent theory-experiment fit ( $R_{\min}=0.055$ ) and a database  $\Delta E=1050$  eV. Yet, we assume that this residual fcc stacking comes from the first bilayer still visible to the LEED electrons between the pyramid-shaped islands displayed in Fig. 4(a).

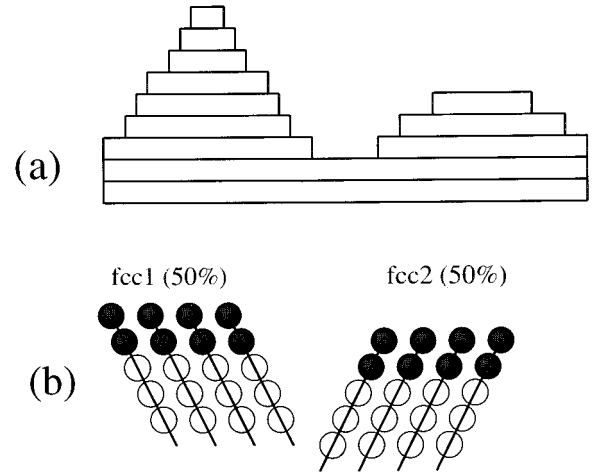


FIG. 4. Schematic structures of the epitaxial film (a) 5 ML Co/Cu(111) and the sandwich system (b) 2 ML Cu/5 ML Co/Cu(111). In (a) domains with different heights are indicated according to the height distribution seen in the STM. In (b) the copper substrate is omitted because LEED provides no information about it due to electron attenuation (symbols as in Fig. 2).

The quantitative structural parameters are given in Table III and experimental and best-fit model spectra are compared in Fig. 5(a). It appears that the in-plane lattice parameter—which was again also varied, but can be determined only as an average over the different layers weighted by the electron attenuation—is reduced to  $a_p \approx 2.51$  Å. This is the relaxed bulk value of Co. Of course, crystallographic defects such as, e.g., dislocations, must develop to allow for such a change of  $a_p$  with growing film thickness.

##### B. The 2 ML Cu/5 ML Co/Cu(111) sandwich

As the 5 ML Co/Cu(111) film turned out to be predominantly hcp stacked, we deposited only two further monolayers of copper in order to check whether or not such a small amount of copper would continue this stacking and whether or not it would leave the cobalt stacking unaffected. The LEED pattern of the sandwich exhibits practically ideal sixfold symmetry and so only models consistent with that needed to be tested. Figure 6 displays four possible models, whereby in the models in Fig. 6(a) the hcp stacking on the two terraces is continued with (right) and without (left) stacking faults. Similarly, the models in Fig. 6(b) stand for

TABLE III. Best-fit structural parameters for the epitaxial film 5 ML Co/Cu(111) according to the model given in Fig. 4(a).

	5 ML Co		
	Domains hcp1	Domains hcp2	Domains fcc
Weight (%)	$45 \pm 5$	$45 \pm 5$	$10 \pm 7$
$d_{12}$ (Å)	$1.96 \pm 0.02$	$1.98 \pm 0.02$	$2.04 \pm 0.03$
$d_{23}$ (Å)	$2.04 \pm 0.03$	$2.04 \pm 0.03$	$2.02 \pm 0.05$
$d_{34}$ (Å)	$1.99 \pm 0.05$	$1.99 \pm 0.05$	2.025 (not varied)
$a_p$ (Å)	$2.507 \pm 0.015$	$2.507 \pm 0.015$	$2.507 \pm 0.040$
$R_{\min}$		0.055	
var( $R$ )		0.014	

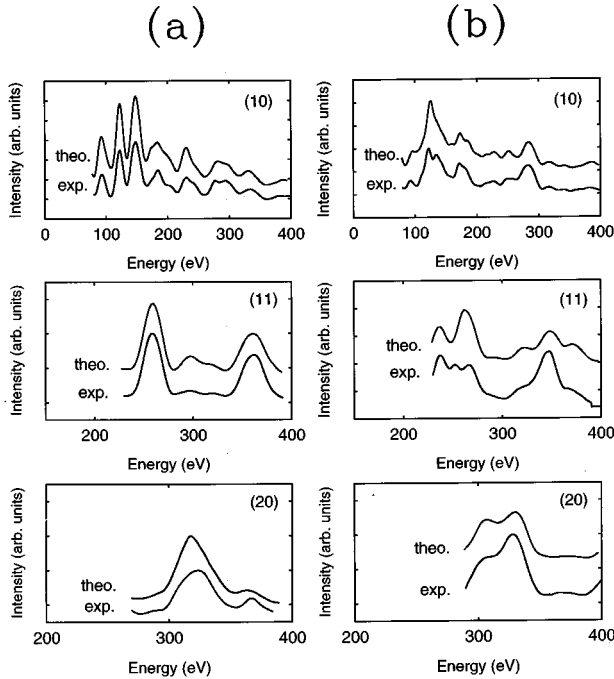


FIG. 5. Comparison of best-fit calculated and experimental spectra for three selected beams of the film (a) 5 ML Co/Cu(111) and the sandwich system (b) 2 ML Cu/5 ML Co/Cu(111).

fcc stacking. The intensity analysis immediately indicates that only the unfaulted fcc stacking [Fig. 6(b), left] comes close to reality. The  $R$  factor  $R=0.31$  for that stacking sequence together with the variance  $\text{var}(R)=0.07$  allows one to rule out the other models shown. Yet the level of the  $R$  factor is still too high to be satisfying and, by experience with the other systems investigated, leaves room for further structural refinement. As interlayer distances are already optimized, this obviously can only come by changes of the stacking in the underlying cobalt film. In fact, if we allow the stacking of all layers to vary with respect to each other, the

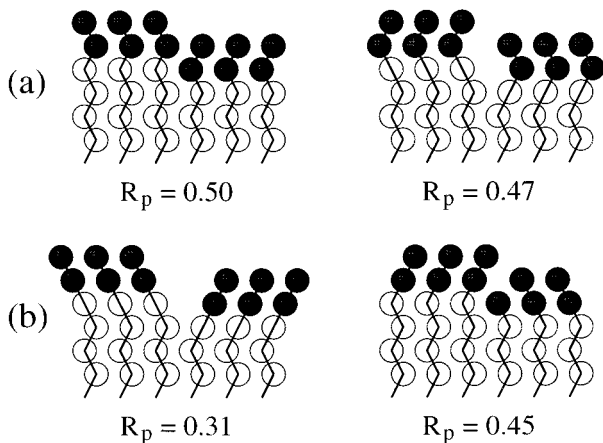


FIG. 6. Possible domains with different stacking producing the experimentally observed sixfold symmetry of the diffraction pattern of 2 ML Cu/5 ML Co/Cu(111) (atomic symbols as in Fig. 2). The Pendry  $R$  factors for each configuration are given for each stacking configuration.

TABLE IV. Best-fit structural parameters for the sandwich 2 ML Cu/5 ML Co/Cu(111) according to the model given in Fig. 4(b).

	2 ML Cu/5 ML Co	
	Domains fcc1	Domains fcc2
Weight (%)	$50 \pm 10$	$50 \pm 10$
$d_{12}$ (Å)	$2.07 \pm 0.03$	$2.07 \pm 0.03$
$d_{23}$ (Å)	$2.07 \pm 0.04$	$2.11 \pm 0.04$
$d_{34}$ (Å)	$2.10 \pm 0.07$	$2.04 \pm 0.06$
$d_{45}$ (Å)	$2.04 \pm 0.10$	$2.08 \pm 0.09$
$a_p$ (Å)	$2.52^{+0.020}_{-0.025}$	$2.52^{+0.020}_{-0.025}$
$R_{\min}$		0.12
$\text{var}(R)$		0.027

best fit results in two equally weighted twinned fcc domains as displayed in Fig. 4(b). The  $R$  factor decreases to a convincingly low level of  $R_{\min}=0.12$ , an agreement between experimental and best-fit data that is also met by the visual comparison of the data as displayed in Fig. 5(b).

Though the minimum  $R$  factor develops for fcc stacking of the full film system, the variance of the  $R$  factor,  $\text{var}(R)=0.027$ , allows one to rule out perturbations of the fcc stacking only within the top five layers, i.e., also in the upper three cobalt layers, which switch from hcp to fcc stacking. Note yet that in order to have a strict fcc stacking, only the Co layer at the interface needs to be shifted due to the Cu capping. Moreover, as given in Table IV the (average) lateral lattice parameter  $a_p$  expands again on copper deposition. Though the latter is not outside the limits of error, it might indicate a reasonable trend, as with further copper deposition the lattice parameter of copper (2.55 Å) should be approached eventually. The interlayer distances agree with each other within the limits of error.

## V. DISCUSSION AND CONCLUSION

The structural results obtained allow one to draw the following scenario: at low coverages of the order of 1.5 ML, the unsandwiched cobalt film grows in double-layer islands with part of the substrate still uncovered and part of the cobalt capped by a copper layer. The atoms of the latter seem to come from the substrate under simultaneous replacement by cobalt, a process that probably mostly takes place near substrate steps.<sup>7</sup> The growth predominantly follows the fcc stacking dictated by copper, in particular the first layer of cobalt. In some small areas stacking faults with respect to fcc stacking exist between the first and second cobalt layers. With further cobalt deposition the film grows with a Poisson distribution of heights changing to hcp stacking. At 5 ML Co nearly full sixfold symmetry of the diffraction pattern results due to hcp domains separated by monoatomic steps. All domains exhibit the relaxed lateral lattice parameter of bulk (0001) cobalt layers,  $a_p = a_p(\text{Co}) = 2.51$  Å.

With sandwiching the thin fcc stacked film by further copper layers, exclusively fcc domains develop. They are partly twinned due to the stacking faults near the lower Co-substrate interface, which remain and are even slightly increased in number by the sandwiching process. This might

be kinetically controlled. However, by sandwiching the thicker and predominant hcp film, its stacking surprisingly is switched to fcc, at least within the information depth of LEED. The full sandwich system exclusively is built up by equally weighted fcc twins that produce the sixfold symmetry of the diffraction pattern. Due to the copper deposition the average in-plane lattice parameter seems to expand again, with the value determined being intermediate between those of copper and cobalt.

Our finding that at low coverages a large part (60%) of cobalt layers is covered by copper is in line with many other investigations (e.g., Refs. 2–4,9,13,14). This observation can easily be explained by the fact that the surface free energy of cobalt ( $2.709 \text{ J/m}^2$ ) is significantly higher than that of copper ( $1.934 \text{ J/m}^2$ ). Yet, our results indicate that copper not only moves to the top by these thermodynamic reasons but is dissolved from the substrate and possibly replaced by cobalt atoms. Of course, the cobalt deposition must be slow enough to allow for both the substitution process and the copper diffusion to the top. It has been argued that at room temperature a deposition rate of  $>30 \text{ ML/min}$  would prohibit diffusion of copper into and on top of the film.<sup>9</sup> Indeed, with about  $1 \text{ ML/min}$  our experiments are well below this limit. Obviously, with more and more cobalt deposited, the diffusion of copper on top becomes more unlikely until with  $5 \text{ ML Co}$  deposited no Cu is detected at the external surface by low-energy AES peaks.

The unusually good fit between experimental and best-fit model intensities in our analyses allows one to determine the layer stacking in a rather detailed way. It appears that to a large extent the fcc substrate dictates cobalt to continue the fcc stacking in the very beginning of the film growth. In particular the first cobalt layer exclusively follows the copper stacking. Yet, the spontaneous formation of stacking faults between the first and second cobalt layers apparently cannot be avoided. The fact that they develop only in domains uncapped by copper confirms the fcc stabilizing influence of copper. Seemingly they initialize the hcp stacking when the film grows thicker. At  $5 \text{ ML}$  there is complete hcp stacking extending down to the substrate. In contrast to the sensitivity of LEED with respect to stacking, we cannot exclude that below the second layer there is intermixing of cobalt and copper. However, in view of the strict hcp stacking found and the observed tendency of copper to stabilize fcc stacking, we feel that this is rather unlikely to happen to a large extent. On the other hand we should emphasize that the fraction of fcc and hcp stacking appears to be also influenced by the crystallographic quality of the substrate, in particular by the density of steps, and by the parameters controlling the growth, as temperature and deposition rate. So, at  $80 \text{ K}$  a larger fraction of hcp Co was reported compared to fcc Co than at room temperature.<sup>3</sup> This indicates the importance of the kinetics of growth. It was also suggested that substrate steps promote fcc stacking.<sup>3</sup> The latter is consistent with our earlier work where we have reported substantial fcc domains even at  $5 \text{ ML}$  coverage.<sup>14</sup>

The unsandwiched  $5 \text{ ML Co}$  film exhibits smaller interlayer distances than expected for a bulk terminated  $\text{Co}(0001)$  crystal, which would exhibit an interlayer distance of  $2.05 \text{ \AA}$ . This is in spite of our result that the lateral lattice parameter has contracted from the copper value ( $2.55 \text{ \AA}$  to that of bulk

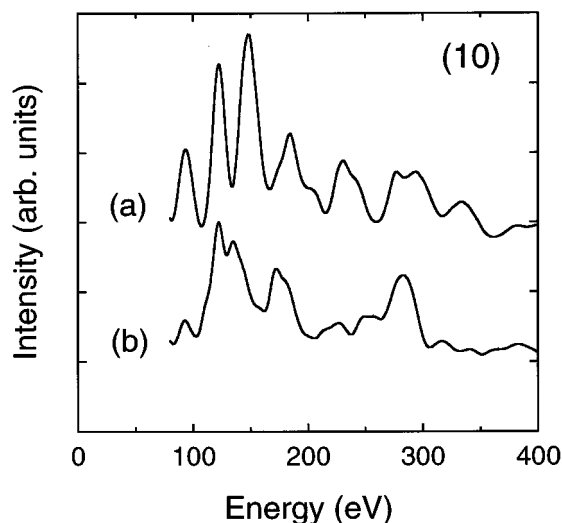


FIG. 7. Comparison of the (10) beam spectra for the  $5 \text{ ML Co/Cu}(111)$  film and the sandwich  $2 \text{ ML Cu}/5 \text{ ML Co/Cu}(111)$ .

cobalt ( $2.51 \text{ \AA}$ ), though this latter finding does not match with results from EXAFS investigations, which report an in-plane next-nearest-neighbor distance of  $2.55 \text{ \AA}$  up to  $8\text{-ML}$  coverage.<sup>11</sup> Yet, the relaxations found fit almost precisely in any case within the limits of error with those determined in an independent LEED structure determination of the clean (0001) surface of a cobalt bulk sample, i.e.,  $d_{12} = 1.99 \pm 0.02 \text{ \AA}$ ,  $d_{23} = 2.05 \pm 0.04 \text{ \AA}$ , and  $d_{34} = 2.01 \pm 0.05 \text{ \AA}$ .<sup>33</sup> This confirms that apart from its surface roughness the epitaxially grown  $5 \text{ ML Co}$  film is already equivalent to the bulk sample's surface with respect to the local crystallographic structure. It is well known that the latter is responsible for the shape of the  $I(E)$  spectra with only little influence of the long-range order.<sup>34</sup>

Yet the most important result of our investigation is the structural behavior of the cobalt film upon deposition of further copper layers, i.e., upon formation of a  $\text{Cu/Co/Cu}$  sandwich. While nothing exceptional happens upon sandwiching the  $1.5 \text{ ML}$  film (fcc stacking simply continues), the stacking of the  $5 \text{ ML}$  film is induced to switch from predominantly hcp to exclusively (twinned) fcc stacking. Figure 7 displays the dramatic change of the spectra [here for the (10) beam, as an example] upon the formation of the sandwich, though the symmetry of the diffraction pattern remains rotationally sixfold. In fact, with only little modification of interlayer distances such a drastic change can only be caused by a change in the stacking sequence. The best theory-experiment fit for the sandwich structure is for a fully fcc stacked film, indicating a stacking change throughout the cobalt film. These findings bear some relevance to our understanding of the frequently reported fcc stacking in  $\text{Co/Cu}(111)$  superlattices. In effect,  $\{5 \text{ ML Co}/3 \text{ ML Cu}\}_{111}$  superlattices grown at room temperature, i.e., precisely the system studied here, were found to be strictly fcc stacked.<sup>17</sup> On the other hand, superlattices with thicker Co layers grown at somewhat elevated temperatures ( $45\text{--}150 \text{ }^\circ\text{C}$ ) are also observed to be fcc,<sup>18,20</sup> which might be due to a floating Cu monolayer constantly segregating to the surface and stabilizing the fcc stacking in the Co layers. However, for the present LEED analysis we admit that electron attenuation allows safe retrieval of stack-

ing only for the top three cobalt layers and the two copper layers. Apparently, this means that a registry shift of only the cobalt layer at the upper Cu-Co interface is sufficient to understand the observed change in the spectra corresponding to a stacking change from *ABABA* in the 5 ML cobalt film to *??ABCab* in the sandwich (the question mark stands for layers about whose registry we cannot safely decide here). Nevertheless, even the registry shift of a single layer means that all atoms of this layer have to move coherently from hcp to fcc sites separated by as much as 1.44 Å. Also, we emphasize that our best fit is for fcc stacking in the entire film, so registry shifts of even deeper layers might be induced too.

At first glance the structural change of the cobalt film upon copper deposition might appear to fit into the general picture of adsorbate-induced restructuring of surfaces, which in recent years has been found to be rather the rule than the exception.<sup>35,36</sup> So, adsorbates generally cause substrate atoms to shift off their equilibrium positions, whereby the amount of the displacement dies away quickly with increasing distance from the surface. Structural changes have been reported also for epitaxial films. So, e.g., the reconstruction found in the full film of several monolayers of Fe grown on Cu(100) is lifted by both further iron deposition<sup>37</sup> and deposition of copper.<sup>38</sup> Yet, in these examples only small (and local) atomic displacements of the order of half an angström are involved in the structural change. Exceptions are with respect to top layer atoms, which may be even locally removed from the surface to form, e.g., a missing row structure.<sup>36</sup> Recently, it has been reported for the growth of Au on Ni(111), which is characterized by a large lattice mismatch, that partial misfit dislocation loops are induced in the substrate.<sup>39</sup> By the formation of vacancies within the substrate, nickel atoms are induced to shift from fcc sites to hcp sites forming a loop of triangular shape and finite size. Apparently, the bonding between gold and nickel, i.e., the interface energy, is optimized.<sup>39</sup> Yet, only a few atoms have to

move. In contrast, the present observation requires the coherent movement of a complete two-dimensional layer whereby, however, we are not in a position to provide quantitative information about its lateral size. As known from STM investigations the film grows in islands and consequently the layers are of finite extension. Obviously, the energy cost for the cobalt layer to switch from hcp to fcc stacking [28 meV atom (Ref. 40)] is overcompensated by the energy gained by the fcc stacked Cu-Co interface configuration.

In conclusion we have shown by quantitative LEED that the initial growth of cobalt on Cu(111), i.e., at 1–2 ML coverage, is via dominant fcc stacking whereby domains with cobalt double layers are formed. Some of them are capped by copper, which is possibly dissolved from the substrate and replaced by cobalt. Yet, while the first cobalt layer exclusively follows the substrate's fcc stacking, some stacking faults between the first and second cobalt layer develop in domains uncapped by copper even at this low coverage. At larger film thicknesses ( $\approx 5$  ML), there is dominant hcp stacking and capping by copper is suppressed. However, the hcp stacking switches back to fcc, forming twinned domains when the cobalt film is sandwiched by further deposition of copper. At least the top cobalt layer undergoes a full registry shift from hcp to fcc sites. Our analyses demonstrate that copper on top of cobalt not only stabilizes the initial fcc stacking of cobalt but even makes it switch back from hcp to fcc when deposited on a thicker Co hcp film.

#### ACKNOWLEDGMENTS

The authors are indebted to the Spanish Ministerio de Educación y Ciencia and Deutscher Akademischer Austauschdienst (DAAD) through the programme "Acciones Integradas" granting scientific exchange visits. The work also has been financially supported by the DGICYT through Grant No. PB94.1527.

<sup>1</sup>L. Gonzalez, R. Miranda, M. Salmerón, J. A. Vergés, and Felix Ynduráin, *Phys. Rev. B* **24**, 3245 (1981).

<sup>2</sup>B. P. Tonner, Z.-L. Han, and J. Zhang, *Phys. Rev. B* **47**, 9723 (1993).

<sup>3</sup>M. T. Kief and W. F. Egelhof, Jr., *Phys. Rev. B* **47**, 10 785 (1993).

<sup>4</sup>Th. Fauster, G. Rangelov, J. Stober, and B. Eisenhut, *Phys. Rev. B* **48**, 11 361 (1993).

<sup>5</sup>V. Scheuch, K. Potthast, B. Voigtländer, and H. P. Bonzel, *Surf. Sci.* **318**, 115 (1994).

<sup>6</sup>J. de la Figuera, J. E. Prieto, C. Ocal, and R. Miranda, *Phys. Rev. B* **47**, 13 043 (1993).

<sup>7</sup>J. de la Figuera, J. E. Prieto, C. Ocal, and R. Miranda, *Surf. Sci.* **307-309**, 538 (1994).

<sup>8</sup>J. Camarero, L. Spendeler, G. Schmidt, K. Heinz, J. J. de Miguel, and R. Miranda, *Phys. Rev. Lett.* **73**, 2448 (1994).

<sup>9</sup>A. Rabe, N. Memmel, A. Steltenpohl, and Th. Fauster, *Phys. Rev. Lett.* **73**, 2728 (1994).

<sup>10</sup>M. Hochstrasser, M. Zurkirch, E. Wetli, D. Pescia, and M. Erbudak, *Phys. Rev. Lett.* **50**, 17 705 (1994).

<sup>11</sup>P. Le Fevre, H. Magnan, O. Heckmann, V. Briois, and H.

Chandesris, *Phys. Rev. B* **52**, 11 462 (1995).

<sup>12</sup>P. Le Fevre, H. Magnan, and D. Chandresris, *Surf. Sci.* **352-354**, 923 (1996).

<sup>13</sup>J. de la Figuera, J. E. Prieto, G. Kostka, S. Müller, C. Ocal, R. Miranda, and K. Heinz, *Surf. Sci.* **349**, L139 (1996).

<sup>14</sup>S. Müller, G. Kostka, T. Schäfer, J. de la Figuera, J. E. Prieto, C. Ocal, R. Miranda, K. Heinz, and K. Müller, *Surf. Sci.* **352-354**, 46 (1996).

<sup>15</sup>K. Le Dang, P. Veillet, Hui He, F. J. Lamelas, C. H. Lee, and Roy Clarke, *Phys. Rev. B* **41**, 12 902 (1990).

<sup>16</sup>H. A. M. de Gronckel, K. Kopinga, W. J. M. de Jonge, P. Panisod, J. P. Schillé, and F. J. A. den Broeder, *Phys. Rev. B* **44**, 9100 (1991).

<sup>17</sup>J. P. Renard, P. Beauvillain, C. Dupas, K. Le Dang, P. Veillet, E. Vélú, C. Marlière, and D. Renard, *J. Magn. Magn. Mater.* **115**, L147 (1992).

<sup>18</sup>G. R. Harp, S. S. P. Parkin, R. F. C. Farrow, R. F. Marks, M. F. Toney, Q. H. Lam, T. A. Rabedeau, and R. J. Savoy, *Phys. Rev. B* **47**, 8721 (1993).

<sup>19</sup>F. J. Lamelas, C. H. Lee, Hui He, W. Vavra, and Roy Clarke, *Phys. Rev. B* **40**, 5837 (1989).



- <sup>20</sup>P. Bödeker, A. Abromeit, K. Bröhl, P. Sonntag, N. Metoki, and H. Zabel, *Phys. Rev. B* **47**, 2353 (1993).
- <sup>21</sup>K. Le Dang, P. Veillet, E. Vélú, S. S. P. Parkin, and C. Chappert, *Appl. Phys. Lett.* **63**, 108 (1993).
- <sup>22</sup>H. Ascolani, J. R. Cerda, P. L. de Andres, J. J. de Miguel, R. Miranda, and K. Heinz, *Surf. Sci.* **345**, 320 (1996).
- <sup>23</sup>In Refs. 13 and 14 a copper substrate with non-negligible density of steps was used. Therefore, at 1.5 ML more and at 5 ML still dominating fcc stacking was found.
- <sup>24</sup>K. Müller and K. Heinz, in *The Structure of Surfaces*, Springer Series in Surface Sciences Vol. 2, edited by M. A. Van Hove and Y. Tong (Springer, Berlin, 1986), p. 105.
- <sup>25</sup>K. Heinz, *Prog. Surf. Sci.* **27**, 239 (1988).
- <sup>26</sup>K. Heinz, *Rep. Prog. Phys.* **58**, 637 (1995).
- <sup>27</sup>J. B. Pendry, *J. Phys. C* **13**, 937 (1980).
- <sup>28</sup>J. B. Pendry, *Low Energy Electron Diffraction* (Academic Press, London, 1974).
- <sup>29</sup>M. A. Van Hove and S. Y. Tong, *Surface Crystallography by LEED* (Springer, Berlin, 1979).
- <sup>30</sup>*American Institute of Physics Handbook*, edited by E. Gray (McGraw-Hill, New York, 1972).
- <sup>31</sup>M. Kottcke and K. Heinz, *Surf. Sci.* (to be published).
- <sup>32</sup>P. Stoltze and J. K. Nørskov, *Phys. Rev. B* **48**, 5607 (1993).
- <sup>33</sup>J. E. Prieto, Ch. Rath, S. Müller, R. Miranda, and K. Heinz, *Verhandl. DPG (VI)* **32**, 885 (1997).
- <sup>34</sup>K. Heinz, U. Starke, and F. Bothe, *Surf. Sci. Lett.* **243**, L70 (1991); K. Heinz, *Phys. Status Solidi A* **146**, 195 (1994).
- <sup>35</sup>K. Heinz, *Surf. Sci.* **299/300**, 433 (1994).
- <sup>36</sup>NIST Surface Structure Database 2.0 (1995) (Nat. Inst. Stand. Technol., Gaithersburg, MD, U.S.A.).
- <sup>37</sup>K. Heinz, P. Bayer, and S. Müller, *Surf. Rev. Lett.* **2**, 89 (1995).
- <sup>38</sup>H. Magnan, D. Chanderiss, B. Vilette, O. Heckmann, and J. Lecante, *Phys. Rev. Lett.* **67**, 859 (1991).
- <sup>39</sup>J. Jacobsen, L. Pleth Nielsen, F. Besenbacher, I. Stensgaard, E. Lægsgaard, T. Rasmussen, K. W. Jacobsen, and J. K. Nørskov, *Phys. Rev. Lett.* **75**, 489 (1995).
- <sup>40</sup>P. M. Marcus and V. L. Moruzzi, *J. Appl. Phys.* **63**, 4045 (1988).